GLIA 57:194–206 (2009)

HIV-1 Tat and Morphine Have Interactive Effects on Oligodendrocyte Survival and Morphology

KURT F. HAUSER,[1,2] YUN KYUNG HAHN,[3] VALERIYA V. ADJAN,[4] SHIPING ZOU,[3] SHREYA K. BUCH,[4] AVINDRA NATH,[5] ANNADORA J. BRUCE-KELLER,[6] AND PAMELA E. KNAPP[1,2,3]*

[1]*Department of Pharmacology and Toxicology, Virginia Commonwealth University, Richmond, Virginia*
[2]*Institute for Drug and Alcohol Studies, Virginia Commonwealth University, Richmond, Virginia*
[3]*Department of Anatomy and Neurobiology, Virginia Commonwealth University, Richmond, Virginia*
[4]*Department of Anatomy and Neurobiology, University of Kentucky College of Medicine, Lexington, Kentucky*
[5]*Department of Neurology, The Johns Hopkins University School of Medicine, Baltimore, Maryland*
[6]*Division of Basic Research, Pennington Biomedical Research Center, Baton Rouge, Louisiana*

KEY WORDS
AIDS; opioid; heroin; drug abuse; glial cell; neuroAIDS; transgenic; cell death; myelin

ABSTRACT
Human immunodeficiency virus (HIV)-infected individuals who abuse opiates show faster progression to AIDS, and enhanced incidence of HIV-1 encephalitis. Most opiates with abuse liability are preferential agonists for μ-opioid receptors (MORs), and MORs are expressed on both neurons and glia, including oligodendrocytes (OLs). Tat, gp120, and other viral toxins, cause neurotoxicity *in vitro* and/or when injected into brain, and co-exposure to opiates can augment HIV-1 protein-induced insults to both glial and neuronal populations. We examined the effects of HIV-1 Tat +/− opiate exposure on OL survival and differentiation. *In vivo* studies utilized transgenic mice expressing $Tat_{1\text{-}86}$ regulated by an inducible glial fibrillary acidic protein promoter. Although MBP levels were unchanged on immunoblots, certain structural and apoptotic indices were abnormal. After only 2 days of Tat induction, OLs showed an upregulation of active caspase-3 that was enhanced by morphine exposure. Tat also upregulated TUNEL staining, but only in the presence of morphine. Tat significantly reduced the length of processes in Golgi–Kopsch impregnated OLs. A greater proportion of cells exhibited diminished or aberrant cytoplasmic processes, especially when mice expressing Tat were co-exposed to morphine. Collectively, our data show that OLs *in situ* are extremely sensitive to effects of Tat +/− morphine, although it is not clear if immature OLs as well as differentiated OLs are targeted equally. Significant elevations in caspase-3 activity and TUNEL labeling, and evidence of increased degeneration/regeneration of OLs exposed to Tat +/− morphine suggest that toxicity toward OLs may be accompanied by heightened OL turnover.

INTRODUCTION

The central nervous system (CNS) is extremely vulnerable to toxicity induced by the human immunodeficiency virus (HIV). HIV encephalitis (HIVE) and neurological complications are a common side effect of AIDS. Before the advent of highly active antiretroviral therapy (HAART), an estimated 10–30% percent of patients experienced full blown HIV-associated dementia (HAD) (Anthony and Bell, 2008; Ghafouri et al., 2006; Kandanearatchi et al., 2003). The use of antiretrovirals and protease inhibitors initially reduced the incidence of HIVE and HAD, and changed the pattern of neurological disabilities and psychological impairment (Cysique et al., 2004; Gonzalez et al., 2002; Gonzalez-Scarano and Martin-Garcia, 2005). However, longer patient survival times and selection of more highly virulent and resistant forms of the virus have resulted in a recent increase in HIVE severity and prevalence (Ances and Ellis, 2007; Anthony and Bell, 2008; Ghafouri et al., 2006; Langford et al., 2003; Neuenburg et al., 2002). Since neurons themselves are not virally infected, neuropathological changes are likely due to combined direct effects of viral proteins on neurons, and indirect inflammatory processes mediated by infected microglia/macrophages or changes in astroglial function. Many studies, including some from our laboratories, show that neurons are either directly or indirectly targeted by HIV viral proteins including gp120, Tat, Nef, Rev, and Vpr (Aksenov et al., 2003; Bonavia et al., 2001; Fitting et al., 2008; Gurwell et al., 2001; Jana and Pahan, 2004; Jones et al., 2007; Kim et al., 2003; Kruman et al., 1998; Lipton, 1997; Nath et al., 1996, 2000; Patel et al., 2000; Singh et al., 2004; Trillo-Pazos et al., 2000). However, only a subset of patients present with symptoms of neuroAIDs, and the onset of those symptoms usually occurs as a relatively late manifestation of the disease process. This suggests that more subtle and indirect insults over a longer time period may be quite important in causing neuronal dysfunction and/or death.

One exacerbating factor in HIVE development appears to be the concurrent exposure to opiate drugs of abuse. HIV-infected individuals who also inject opiate drugs

Grant numbers: NIH: P01 DA19398 + R01 DA24461.

*Correspondence to: Pamela E. Knapp, Department of Anatomy and Neurobiology, MCV Campus, Virginia Commonwealth University, 1217 East Marshall St. Rm. 411, PO Box 980709, Richmond, VA 23298-0709, USA.
E-mail: peknapp@vcu.edu

Received 11 February 2008; Accepted 29 June 2008

DOI 10.1002/glia.20746

Published online 28 August 2008 in Wiley InterScience (www.interscience.wiley.com).

show accelerated progression to clinical AIDS and to HIVE, which may lead to HAD (Anthony et al., 2008; Bell et al., 2006; Burdo et al., 2006; Hauser et al., 2007; Kopnisky et al., 2007). Opiates with abuse liability largely target the μ-opioid receptor (MOR), which is widely expressed both peripherally and in the CNS. Interactions between opiates and HIV or related viruses and viral proteins appear to directly accelerate viral replication under many conditions (Li et al., 2003; Noel and Kumar, 2006; Peterson et al., 2004; Schweitzer et al., 1991; Suzuki et al., 2002). Progression to AIDS and HIVE is undoubtedly advanced by MOR-signaling on cells of the peripheral immune system, whose function is altered by chronic opiate exposure (Carr and France, 1993; Donahoe and Falek, 1988; Nath et al., 2002; Peterson et al., 1993; Vallejo et al., 2004). However, there is a substantial evidence in several disease models that both neurons and glia, as well as immune cells in the brain, are directly affected by co-exposure to opiates and HIV in a manner that would ultimately lead to greater compromise of CNS function. *In vitro*, concurrent exposure to morphine promotes Tat-induced striatal neuron death and also destabilizes Ca^{2+}-signaling in astroglia, leading to enhanced secretion of proinflammatory chemokines and cytokines and enhanced macrophage/microglial migration (El-Hage et al., 2005, 2006b; Gurwell et al., 2001). Similar effects can be observed in some studies with co-exposure to gp120 and morphine (Hu et al., 2005; Mahajan et al., 2005; Turchan-Cholewo et al., 2006). *In vivo*, the intrastriatal injection of Tat into morphine-treated mice results in astrogliosis and increased microglial numbers, as well as an overall upregulation in the percentage of cells expressing MORs (El-Hage et al., 2006a).

The present study explores the possibility that oligodendrocytes (OLs), in addition to other CNS cells, may be targets of lethal or sublethal effects of HIV-1 Tat. Myelin pallor has been described by neuropathology and on MRI scans from some HIV patients (Cherner et al., 2002; Glass et al., 1993; Gray et al., 1992, 1996; Lanjewar et al., 1998; McArthur et al., 1989; Schwartz and Major, 2006), and although this has been thought to be a consequence of endothelial damage and increased blood brain barrier permeability, the direct and/or secondary effects of HIV proteins on OLs have not been studied in detail. An earlier study reported no changes in myelin basic protein levels and no demyelinated regions in brains of patients with HIV dementia (Power et al., 1993). However, there are more subtle changes in myelin, in axon–myelin interactions, or in OL function that might contribute to neuron dysfunction. Additionally, since OLs express MORs and other classes of opioid receptors both *in vivo* and *in vitro* (Knapp et al., 1998, 2001; Stiene-Martin et al., 2001; Tryoen-Toth et al., 2000), and since opioid receptors modulate OL growth and viability *in vitro* (Knapp and Hauser, 1996; Knapp et al., 1998, 2001), we explored the combined effects of Tat and opiate exposure. *In vivo* studies utilized a transgenic mouse in which HIV-1 $Tat_{1\text{-}86}$ is produced in astroglia under control of a doxycycline (DOX)-induced promoter. We report that Tat exposure in combination with morphine can variably affect indices of OL phenotype and well-being. Tat exposure alone alters process outgrowth and caspase-3 expression in OLs within the striatum and/or corpus callosum. Terminal dUTP nick end labeling (TUNEL) is increased when Tat is delivered concurrently with morphine. Some effects are exacerbated by co-exposure to morphine, while others are lessened. Thus OLs, in addition to neurons and other CNS glia, may be primary or secondary targets of Tat and opioid toxicity.

METHODS

Tissue Culture

Progenitor cultures containing OL precursors were prepared from striatum of embryonic day 14-15 (E14-15) mouse pups using modifications of a previously published technique (Khurdayan et al., 2004). Briefly, timed pregnant ICR dams (Charles River, Boston, MA) were deeply anaesthetized with halothane and pups were removed from the uterus. The striata from 10 to 12 pups were dissected from the cortex, finely minced, and incubated with 5 mL of DNAse (0.015 mg/mL) in Dulbecco's Modified Eagle's Medium without additives (15 min, 37°C). Tissue was triturated through a 5 mL-pipette, centrifuged (5 min, 800 rpm), suspended in 5 mL-progenitor maintenance medium (1:1 DMEM/F12; insulin (25 μg/mL); transferrin (100 μg/mL); progesterone (20 nM); putresceine (60 μM); sodium selenite (30 nM); all from Sigma), and filtered through 70-μm pore nylon mesh. Resulting cells were counted, centrifuged, and resuspended in the same medium. After a second filtration, the supernatant was plated on either poly-L-lysine coated T25 culture flasks for RT-PCR (3×10^6 total cells) or poly-L-lysine coated glass coverslips for immunostaining (3×10^5 cells in 150 μL). Cultures containing more mature OLs and used for immunostaining were isolated similarly, grown in progenitor maintenance medium for one week, and gradually switched to differentiation medium (DMEM with 5 μg/mL insulin, 25 μg/mL transferrin, 10 ng/mL biotin, 5 ng/mL sodium selenite, and 6.0 mg % glucose, and antibiotics). Some cultures were subsequently treated with $Tat_{1\text{-}86}$ (ImmunoDiagnostics, Woburn, MA; 100 nM), morphine sulphate (NIDA Drug Supply System, Rockville, MD; 500 nM), Tat + morphine, or Tat + morphine + naloxone (NIDA Drug Supply System) 1.5 μM for 24 h prior to fixation and immunostaining for active caspase-3 and OL markers. All treatments were applied simultaneously in prewarmed medium.

Opioid Receptor PCR

Nonquantitative RT-PCR was used to document the presence of mRNA for each major opioid receptor in OL progenitor cultures. At 2 and 5 days after plating, progenitors were harvested by scraping into ice-cold, deion-

ized water from culture plates. Total RNA was isolated using GenElute™ Mammalian Total RNA kit (Sigma). cDNA was synthesized from 2 μg of total RNA using the High-Capacity cDNA Archive Kit (Applied Biosystems, Warrington, UK) per manufacturer's instructions. Primers for MOR (forward, 5′-CCGCAGCAAGCATTCAGAA-3′; reverse, 5′ GCCATCAACGTGGGACAA 3′), KOR (forward, 5′-GAGCACCAATAGAGTTAGAAA-3′; reverse, 5′-CCTGGAGAACAATAAGAAGAC-3′), and DOR (forward, 5′-GCGTGTCACTGCCTGCAC-3′; reverse, 5′-TGGCCTCTGGATCACTTCACT-3′) were used to assay opioid receptor expression. 18S mRNA was assayed as a control (forward, 5′-CACTTGTCCCTCTAAGAAGTTG-3′; reverse, 5′-GACAGGATTGACAGATTGATAG-3′).

Opiate and Tat Delivery *In Vivo*

In vivo studies utilized a transgenic mouse engineered to express the HIV-1 $Tat_{1\text{-}86}$ protein in astrocytes in a doxycyline-inducible manner. As previously described (Bruce-Keller et al., 2008), mice expressing the Tat gene under control of a tet responsive element (TRE) in the pTREX vector (Clonetech, Mountain View, CA) were crossed with mice engineered to express the glial fibrillary acidic protein (GFAP) promoter driving the reverse tetracycline transactivator (RTTA). The inducible Tat transgenic mice (Tat^+ mice) used in these studies express both GFAP-RTTA and TRE-Tat genes, while the control mice (Tat^- mice) express only the GFAP-RTTA gene. Individual animals were genotyped using RNA isolated from ear clip samples, by standard PCR procedures previously described (Bruce-Keller et al., 2008). Tat-induction was obtained by replacing standard chow with a formulation containing DOX at 6 mg/g (Harlan, Indianapolis, IN). Some control groups were also fed DOX-containing chow to control for nonspecific actions of DOX intake.

Morphine was delivered by 25 mg, timed-release pellets (NIDA Drug Supply System) implanted subcutaneously in the subscapular region under aseptic conditions using isoflurane anesthesia. Sham pellets were similarly implanted as controls. The 25-mg morphine pellets reportedly deplete at a rate of 5 mg/day, yet steady state levels of morphine, measured in ng/mL plasma or ng/g brain tissue reflect lower availability, probably due to the balance of delivery and metabolism [see, e.g., (Feng et al., 2006)]. Both C3HeB and C57Bl mice reportedly tolerate delivery from 75 mg/5 day morphine pellets (Peart and Gross, 2004; Rahim et al., 2003). Less than 5% of the mice in our studies died, and there was no relationship between morphine-induced toxicity and either genotype or DOX administration.

In experiments lasting for a total of 7 days, opioid and control pellets were replaced after 5 days. Naltrexone (NTX) was administered via an Alzet mini-pump (1007D) implanted in the same region. 600 mg/mL NTX (NIDA Drug Supply System) was prepared in 50% DMSO, a standard vehicle for mini-pump delivery (Arnot et al., 1996). 100 μL total volume was loaded per mini-pump, delivering 0.5 μL/h for up to 7 days. Pumps containing 50% DMSO and sterile saline were used as NTX controls. For studies where mice were exposed to both opioids and Tat, mice were given the DOX feed starting on the night before opioid treatment in order for blood levels of DOX to stabilize. For histological studies, mice were deeply anaesthetized with halothane prior to perfusion with Zamboni's fixative (2% paraformaldehyde, pH 7.4, with 0.15% picric acid).

Immunostaining and Quantification *In Vivo*

After perfusion, brains were removed and postfixed in fresh fixative overnight. Brains were hemisected, rinsed several times and overnight in 15 mL changes of phosphate-buffered saline, cryopreserved through graded sucrose solutions (10 and 25%), embedded in Tissue Tek OCT compound (Sacura Finetek, Torrance, CA), and stored at –80°C. 12-μm frozen sections containing the corpus callosum were thaw-mounted on SuperFrost Plus slides (VWR Scientific, West Chester, PA) and processed for immunostaining. Sections were double-stained sequentially for APC (adenomatous polyposis coli), followed by immunostaining for active caspase-3 or terminal deoxynucleotidyl transferase-mediated dUTP-biotin nick-end labeling (TUNEL) using fluorescent markers. APC is a tumor suppressor gene whose mutation is linked to forms of colon cancer, but which is also expressed specifically in OL cell bodies in the brain (Bhat et al., 1996). It is especially useful for unambiguous quantification of cell numbers since it does not stain myelin. Sections were rinsed and permeabilized with 0.3% Triton X-100 in phosphate-buffered saline containing 5% normal goat serum and 0.1% bovine serum albumin for 30 min. APC/CC-1 antibody (Oncogene, San Diego, CA; 5 mg/L or 1:20) was applied for 1 h at room temperature, followed by visualization with goat anti-mouse second antibody conjugated to Oregon Green 488 (Molecular Probes; 1:250; 1 h; room temperature). In some cases, APC staining was followed by overnight incubation with affinity-purified rabbit anti-human/mouse active caspase-3 antibody (R&D Systems, Minneapolis, MN; 1:2,000, 4°C). This antibody detects amino acids 163–175 of the p17 subunit of caspase-3, but does not detect or poorly detects the precursor form. Anti-caspase-3 was visualized with goat anti-rabbit IgG conjugated to CY-3 (Jackson ImmunoResearch, West Grove, PA). In other sections, APC staining was combined with TUNEL labeling to detect *in situ* DNA fragmentation using the TACS2-TdT Apoptosis Detection Kit (Trevigen, Gaithersburg, MD), per manufacturer's directions. Lastly, immunostained sections were incubated with Hoechst 33342 dye (1:20,000) for identification of all nuclei (Molecular Probes), mounted in ProLong Gold antifade reagent (Molecular Probes), and dried for 8 h in the dark. Sections were stored dessicated at –80°C and used for quantitation within 2 months. No nonspecific binding was observed when the primary antibodies were omitted.

APC^+ OLs were identified in the corpus callosum in the region of the cingulum at 63×. The first 100 APC^+ cells per section that were clearly distinct from neighboring cells were assessed for either caspase-3 or TUNEL staining depending on the experiment. Cells were counted only if the entire nucleus was stained with Hoechst. Two separate sections at least 40-μm apart were examined per animal and averaged in $N = 4–5$ animals per experimental group. The relative percentage of OLs expressing active caspase-3 or TUNEL was calculated and compared between treatment and control groups. Stereological techniques were not used in this study since we were interested in the relative response of OLs within the population.

Immunostaining and Quantification *In Vitro*

In some experiments, cultured cells were double-immunostained for μ, δ, or κ-opiate receptors and olig-2, a basic helix-loop-helix (bHLH) transcription factor that is required for OL lineage specification in the brain and spinal cord (Ligon et al., 2006; Woodruff et al., 2001). In other experiments, we double-stained cells using O_4 antibody and an antibody to active caspase-3. O_4 antibody detects sulfatide (Sommer and Schachner, 1982), a sulfated galactocerebroside specifically expressed by immature and mature OLs in the brain. In terms of developmental expression, olig-2 is an earlier marker than sulfatide, but both are also found in mature OLs. Cells were immunostained using O_4 hybridoma supernatant harvested in our laboratory (1:2, 20 min, 4°C), then visualized with goat anti-mouse IgM-FITC (Jackson ImmunoResearch, 1:250, 20 min, 4°C) prior to fixation in 4% paraformaldehyde for 10 min. The antibody to active caspase-3 was then applied and visualized as described for the tissue sections above. The effect of Tat and/or opioids on the activation of caspase-3 in OLs was quantified after 24 h of treatment. At least 100 04^+ cells were selected randomly on duplicate coverslips from each treatment group in $N = 3$ different cultures, then assessed for active caspase-3 immunostaining.

Golgi–Kopsch Impregnation/OL Process Measurement

Whole forebrains ($N = 4–8$ for each treatment) were impregnated after 7 days of DOX and/or opioid treatment using a modified Golgi–Kopsch procedure that randomly impregnates neurons and glia (Hauser et al., 1989). Briefly, mice were deeply anesthetized by halothane inhalation and euthanatized by intracardiac perfusion with 2% potassium dichromate and 5% glutaraldehyde. Perfused forebrains were isolated and immersed in 2% potassium dichromate and 5% glutaraldehyde (v/v) in the dark at room temperature. The ratio of dichromate solution to tissue volume was at least 50:1. After 5 days, the tissue was rinsed twice in ultrapure water three times, blotted dry after each rinse, and placed in aqueous 0.75% silver nitrate solution for 5 days in the dark (50:1 fluid to tissue volume ratio). Intact forebrains were infiltrated with graded sucrose solutions (10, 20, and 30% sucrose in 0.75% silver nitrate) for 24-h periods, then embedded in Tissue Tec OTC compound, frozen on dry ice, and stored at –80°C. Serial, coronal sections were cut at 120 μm, thaw-mounted on Fisher Superfrost-Plus microscope slides, dehydrated through graded ethanols, cleared in xylene, and mounted in Permount (Fisher Scientific, Waltham, MA). Nonmetallic handling devices were used throughout. All slides were quantified by an individual unaware of the treatment group.

Although the Golgi procedure randomly impregnates neurons and glia, additional criteria were used to determine whether an OL was sampled, and OLs that fulfilled all of the following criteria were arbitrarily selected and analyzed: (1) OLs had to be discernable from other cell types. This included having the unique cellular morphology characteristic of OLs (e.g., small, ~10 μm-diameter cell body, myelin-forming cytoplasmic processes aligned along white matter tracts) and a location appropriate for OLs (e.g., associated with focal striatal white matter bundles, or in the corpus callosum adjacent to the striatum); (2) OLs had to be entirely impregnated throughout all processes; (3) OLs had to be located in the middle of the 120-μm section thickness so that they could be measured in their entirety, and (4) OL cytoplasmic processes could not overlap those from nearby neurons or glia, and could not contact blood vessels. A MicroBrightfield Neurolucida System (Williston, VT) configured with a Zeiss Axiomat microscope and *x*, *y*, and *z*-axes stage-encoder was used to measure and analyze OL processes in 3-dimensions. For individual OLs, estimates of: (i) total process length, (ii) the number of intervening segments (number of processes + number of times they branch), and (iii) mean segment length (total length/number of process segments) were obtained. We estimated the total process length for each individual OL. At least 20 OLs were measured from each animal, with 4–8 animals/group. Photomicrographs were obtained using a Nikon Diaphot microscope with 100× oil-immersion objective and Spot 2 digital camera (Diagnostic Instruments, Sterling Heights, MI) or a Zeiss Axio Observer Z1 microscope with an AxioCam MRm (Carl Zeiss, Inc.), and 63× or 100× oil-immersion objective. In the case of the Zeiss Axio Observer microscope images, multiple z-stack images were typically acquired through the same OL at 0.25–0.45 μm intervals. Different z-plane images from the same OL were projected into a single, sharp 2-dimensional image using the Extended Focus Module (AxioVision 4.6.3, Carl Zeiss, Thornwood, NY) with "Normal" alignment and the "Wavelets" algorithm to compress the images (Fig. 5D,E,H,I,L,M).

Immunoblotting

Total proteins were extracted from cortical tissue by homogenization in RIPA buffer (50 mM Tris pH 7.4,

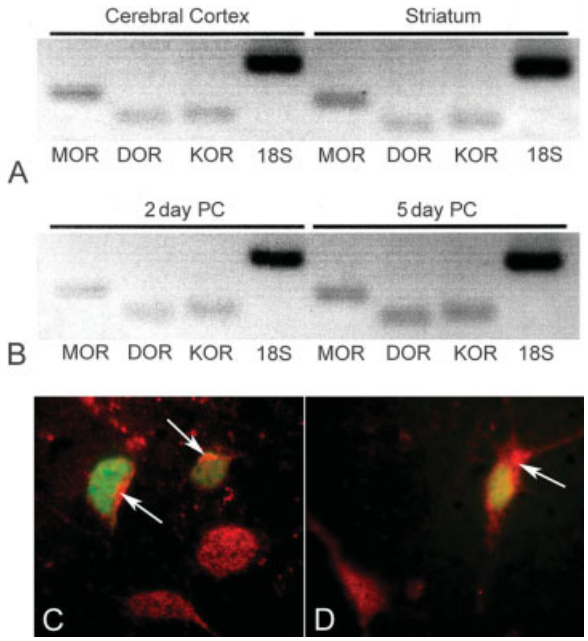

Fig. 1. OL progenitors express opioid receptors. (**A**, **B**) Real time RT-PCR detection of mRNA for MOR, DOR, and KOR in (A) striatum and cerebral cortex from embryonic day 15 (E15) mice, and in (B) progenitor cells (PC) from E15 stratium after 2 and 5 days in culture. (**C**, **D**) Progenitors in E15 stratial cultures stained for MOR (red) and Olig-2 (green), a transcription factor indicating commitment to the OL lineage in these cultures. Arrows indicate double-labeled cells, many of which are Olig-2$^-$, showing that MORs are expressed in both committed and multipotential cells.

150 mM NaCl, 1% Nonidet, 0.5% deoxycholic acid, 0.1% SDS, one tablet of protease inhibitors from Roche in 10 mL RIPA). Protein concentration was measured using the BCA Protein Assay Kit (Pierce, Rockford, IL). 20 μg of total protein was separated on 15% Tris-HCl Ready Gels (Bio-Rad, Hercules, CA) and blotted to Hybond-P membrane (Amersham Biosciences, Piscataway, NJ). MBP was detected using a monoclonal antibody that identifies all major isoforms except for 14 kDa (SMI 99, 1:1,000; Covance Research Products, Princeton, NJ). Blots were detected using the ECL-Plus detection system (Amersham) and visualized on a Kodak Image Station 440.

Statistical Analysis

All results, except those for the TUNEL labeling, were analyzed by ANOVA and Duncan's *post hoc* testing using either JMP 5 (SAS, Cary, NC) or StatSoft (Statistica, Tulsa, OK) software. In the case of the TUNEL analysis, Kruskal–Wallis nonparametric ANOVA and *post hoc* multiple comparisons tests were used to assess statistical relevance.

RESULTS

Overall, our results suggest that OLs are extremely sensitive to the effects of HIV-1 Tat exposure, and that the consequences of Tat exposure can be either selectively exacerbated or alleviated by concurrent exposure to morphine.

TABLE 1. Percent of Olig-2$^+$ Cells Expressing μ-, δ-, and κ-Opioid Receptors In Vitro

	2 DIV	5 DIV
MOR	71.2 ± 3.8	72.0 ± 2.9
DOR	67.6 ± 11.9	64.7 ± 4.1
KOR	69.7 ± 9.0	71.4 ± 2.5

Cells were cultured from E14-15 striatum and assessed after 2 or 5 days *in vitro* (DIV). $N = 4$ for MOR; $N = 3$ for DOR and KOR.

Expression of Opioid Receptor Genes in Cells of the OL Lineage

We used RT-PCR and immunocytochemistry to determine whether glial progenitors and immature OLs express opioid receptors. mRNA for MOR, DOR, and KOR was detected in whole tissue samples taken from E15 cerebral cortex and striatum (Fig. 1). We next prepared highly purified glial progenitor cells from E14-15 striatum, and cultured them for 2 or 5 days prior to performing RT-PCR. mRNA for all three receptors was detected at both times in culture (Fig. 1). Since these were mixed progenitors, we used immunohistochemistry to determine the types of receptors expressed in immature cells committed to an OL fate. Double-labeling showed that most immature glia expressing the olig-2 transcription factor also expressed one or more opioid receptors at both 2 and 5 days in culture (Table 1). Many cells that immunostained for opioid receptors did not express olig-2, suggesting that glial precursors at many stages of development could interact with, and be targets of, opioid ligands.

Active Caspase-3 and TUNEL Expression

To determine whether Tat and/or opioid exposure might ultimately affect the survival of OLs, we assessed their effects on two potential indicators of apoptosis—activation of caspase-3 and TUNEL labeling. The calcium-dependent protease caspase-3 is a major effector of programmed cell death. An antibody that detects activated human/mouse caspase-3 was used in combination with markers for OLs both *in vitro* and in frozen sections. Since it is now recognized that caspase-3 may be activated under certain nonlethal conditions, such as during stress, development, or tissue remodeling (Campbell and Holt, 2003; Jarskog et al., 2007; McLaughlin, 2004; Oomman et al., 2004, 2005; Yang et al., 2004a,b), we also evaluated TUNEL labeling as a more certain indicator of nuclear fragmentation and cell death.

We first examined glial progenitor cells that had been in culture under differentiating conditions for 7 days prior to 24-h treatment with exogenous HIV-1 $Tat_{1\text{-}86}$, morphine, Tat + morphine, or Tat + morphine + naloxone. Exposure to Tat or morphine alone increased active caspase-3 expression in O_4^+ cells, and the combination was synergistic (Fig. 2). The exacerbation caused by con-

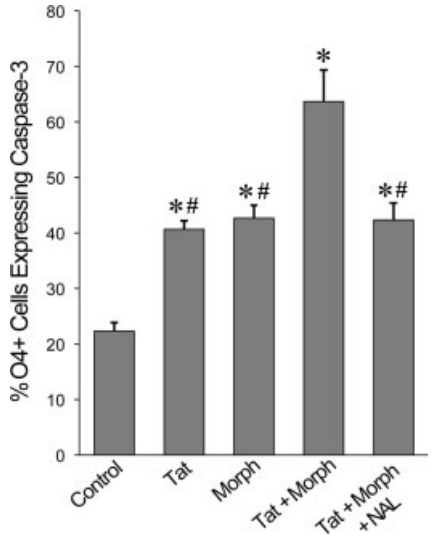

Fig. 2. Tat and morphine (Morph) elevate active caspase-3 expression in cultured OLs. A 24-h exposure to $Tat_{1\text{-}86}$ (100 nM) or morphine (500 nM) alone caused a 2-fold increase in immunohistochemical expression of activated-caspase-3 in O_4^+ OLs. Concurrent exposure to Tat and morphine resulted in an exacerbation of activated caspase-3 expression as compared with either treatment alone. Naloxone (NAL; 1.5 μM) eliminated the Tat + Morph exacerbation, but did not block the effects of morphine alone. *$P \leq 0.005$ vs. control; #$P \leq 0.005$ vs. Tat + Morphine. $N = 3$ separate cultures.

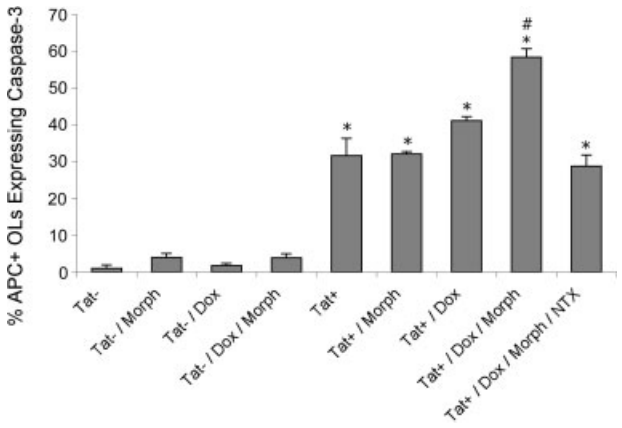

Fig. 3. Active caspase-3 expression is increased in OLs from Tat^+ mice and is enhanced by co-treatment with morphine. Tat^+ and Tat^- mice were treated with combinations of DOX, morphine (Morph), and naltrexone (NTX) for 2 days. Cells of the OL lineage were identified by APC staining within the corpus callosum. The percent of APC^+ OLs expressing active caspase-3 was significantly increased in all Tat^+ groups vs. all Tat^- groups (*$P < 0.01$ vs. all Tat^- groups). Tat^+ mice receiving DOX + morphine showed synergistic toxicity (#$P < 0.01$ vs. all other Tat^+ groups). Simultaneous treatment with NTX blocked the Tat-morphine synergism.

current Tat and morphine exposure was blocked by naloxone, suggesting that the additivity was an opioid-specific response. TUNEL was not examined in cultured cells because of background DNA fragmentation in non-phagocytized cells over time.

Inducible Tat-transgenic mice were used to examine caspase-3 and TUNEL expression in OLs within the CNS. Tat^+ and Tat^- mice were treated with combinations of DOX, morphine, and NTX for 2 days. OLs were

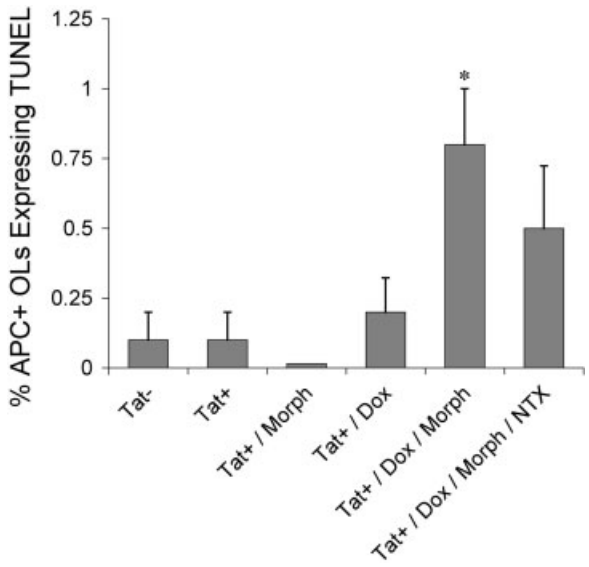

Fig. 4. TUNEL expression is not increased by Tat alone, but is increased in OLs treated with both Tat and morphine. Tat^+ and Tat^- mice were treated with combinations of DOX, morphine (Morph), and naltrexone (NTX) for 2 days. Dying OLs were identified using APC immunostaining and a fluorescent TUNEL marker. Only a small percentage of APC^+ OLs were also $TUNEL^+$ in any of the groups. Cells at this stage of apoptosis are rapidly phagocytized *in vivo*. The percentage of APC^+ cells that are also $TUNEL^+$ was only increased in Tat^+ mice receiving both DOX and morphine treatments, suggesting synergy between the morphine and Tat treatments (*$P \leq 0.03$ vs. Tat^-, Tat^+, Tat^+/Morph, and Tat^+/DOX, nonparametric ANOVA; $N = 5$). The TUNEL levels with NTX treatment were intermediate between the control and the Tat^+/DOX/Morph groups, and were not significantly different from either. Thus NTX at least partially blocked the morphine-induced synergy.

identified by immunostaining with the APC marker. OLs in all groups of Tat^- mice, both untreated mice and those receiving DOX and/or opioid treatments, had low levels of active caspase-3 expression ($\leq$5%) and none of the groups were significantly different from one another (Fig. 3). In contrast, levels of caspase-3 expression were significantly elevated within OLs in all groups of Tat^+ mice. Both DOX-induced and uninduced Tat^+ mice had similarly elevated expression levels, suggesting that the DOX-induced promoter has some constitutive activity, and that caspase-3 activation occurs with even low levels of Tat production. In Tat^+ mice given DOX, concurrent morphine exposure resulted in a significantly increased number of APC^+ OLs expressing active caspase-3 (Fig. 3). However, morphine administration did not exacerbate caspase-3 expression in the uninduced Tat^+ mice, suggesting that opioid-Tat interactive effects on caspase-3 expression must require a threshold level of Tat that was not reached without DOX administration. NTX eliminated Tat + morphine additivity, showing that the caspase-3 response was opioid specific.

TUNEL results were somewhat different. In adjacent sections from the same mice, TUNEL expression was not increased by Tat alone, but was significantly increased in OLs treated with both Tat and morphine (Fig. 4). As would be expected, only a small percentage of APC^+ OLs were also $TUNEL^+$ in any of the groups.

This is because cells at the stage of apoptosis where DNA is damaged are very rapidly phagocytized *in vivo*. Of great interest, the percentage of APC^+ cells that were $TUNEL^+$ was increased after 2 days of DOX treatment, but only in the Tat^+ mice that also received morphine (*$P = 0.03$). NTX at this dose (60 mg/100 μL 50% DMSO) partially blocked morphine-induced synergy. The TUNEL labeling index of the Tat^+/DOX/morphine/NTX group was reduced to a level that was no longer significantly different than Tat^-, Tat^+, Tat^+/DOX, or Tat^+/DOX groups, but at the same time was not different than the Tat^+/DOX/morphine group. This partial blockade of morphine-induced synergy was in contrast to the complete blockade seen with caspase-3 expression.

Oligodendrocyte Morphology and Process Length

Mature OLs typically elaborate multiple processes, each of which has the potential to contact and form myelin around a separate axonal segment. The measurement of total process length per OL is therefore one indication of whether the OL population is phenotypically normal. OLs were impregnated using the Golgi–Kopsch technique (Hauser et al., 1989) to visualize and measure their process network. This staining technique results in random impregnation of the cell body as well as processes of individual neurons and glia and, as can be appreciated from Fig. 5, detailed measurements of process extensions can be made by focusing through the body of the tissue section. Impregnation was done at 7 days after DOX administration, since we initially thought that phenotypic alterations might not occur immediately after the transgene was activated. In OLs from the striatum and adjacent corpus callosum of control mice without the Tat transgene (Tat^-), the average total process length per cell was ~1,000 μm. This length was reduced significantly in mice with the Tat transgene (Tat^+) regardless of the presence of DOX (Fig. 6). Since both the uninduced and the DOX-induced Tat^+ mice showed equivalent reductions in process length, it is likely that the DOX-induced promoter has some constitutive activity and that process outgrowth is quite sensitive to continuous, low levels of Tat production. Evidence of such constitutive activity was also observed in the caspase-3 data (Fig. 3). Morphine appeared to dampen the Tat-induced reductions in process length in Tat^+ mice both with and without DOX. However, the dose of NTX used here did not block the morphine-induced changes in process length.

Figure 5 shows examples of Golgi-impregnated OLs from different genotypes and treatment groups. Large, mature, and well-arborized OLs were present in both Tat^- and Tat^+ mice (e.g., Fig. 5A,B,H,I). However, the Tat^+ groups also had a population of mature OLs with an aberrant phenotype. These abnormal cells were more evident in Tat^+ mice receiving DOX, and especially so when morphine was co-administered. Some OLs had reductions in total number of cytoplasmic processes, and/or stunted or abbreviated processes (Fig. 5F,G,J,L,M). Others had abnormal varicosities along their length or large, club-like cytoplasmic endings that could be several microns in diameter (Fig. 5F,G,I,J,K). Normal OLs typically have a smooth-surfaced round or ovoid cell body (Fig. 5A,C,D), yet in many Tat^+ OLs the cell body was irregular in shape, and/or had a rough, wrinkled appearance (Fig. 5I,J,M). Others had cytoplasmic/myelinating processes that failed to align with processes of other OLs in white matter tracts (Fig. 5C,D,M). Occasional cells were so severally degenerated that their identity could not be determined with certainty, although the size of the soma and location relative to white matter tracts suggested an OL identity. Abnormal OLs did not appear to correlate with a particular subregion of the striatum, but may coincide with heterogeneity in Tat expression among astrocytes since we noted a tendency for aberrant cells to cluster in foci, with otherwise normal appearing OLs in the surrounding areas. OLs with aberrant morphology were only occasionally observed in Tat^- mice, and these abnormal cells might represent normal glial turnover processes (Fig. 5E).

MBP Levels

As an index of overall myelination, levels of MBP protein were assessed by immunoblotting in cortical samples taken from Tat^- and DOX-exposed Tat^+ mice. The Tat^+ mice had received DOX in their drinking water for 4 weeks prior to tissue harvesting. The results therefore reflect the effects of a more prolonged exposure to elevated Tat than other endpoints reported here, and which were taken after 2 days of DOX exposure. Quantitative densitometric analysis of MBP immunoblots from DOX-exposed Tat^+ mice ($n = 4$) and Tat^- mice ($n = 4$) were essentially identical (ratio 1.034) after correction for loading. This suggests that any alterations in myelin integrity that occur with Tat exposure are more subtle than can be detected as the loss of a major myelin protein.

DISCUSSION

Our data indicate that OLs are cellular targets of the HIV-1 Tat protein, both *in vitro* and within the CNS. Findings in culture suggest that some effects could be direct, although it is likely that effects observed in Tat-transgenic mice also have an indirect component. Many, but not all, of these effects are exacerbated by concurrent exposure to morphine. Others, such as increased TUNEL labeling, are only observed in the presence of morphine. Thus, exposure to opioid agonists with abuse potential may have profound effects on the relationships between OLs and neurons/axons in HIV-infected individuals, especially considering the extended time course of the disease process.

Our motive for exploring this issue was to determine whether HIV-1 Tat and opiates might have synergistic effects on OLs, as shown previously by our laboratories

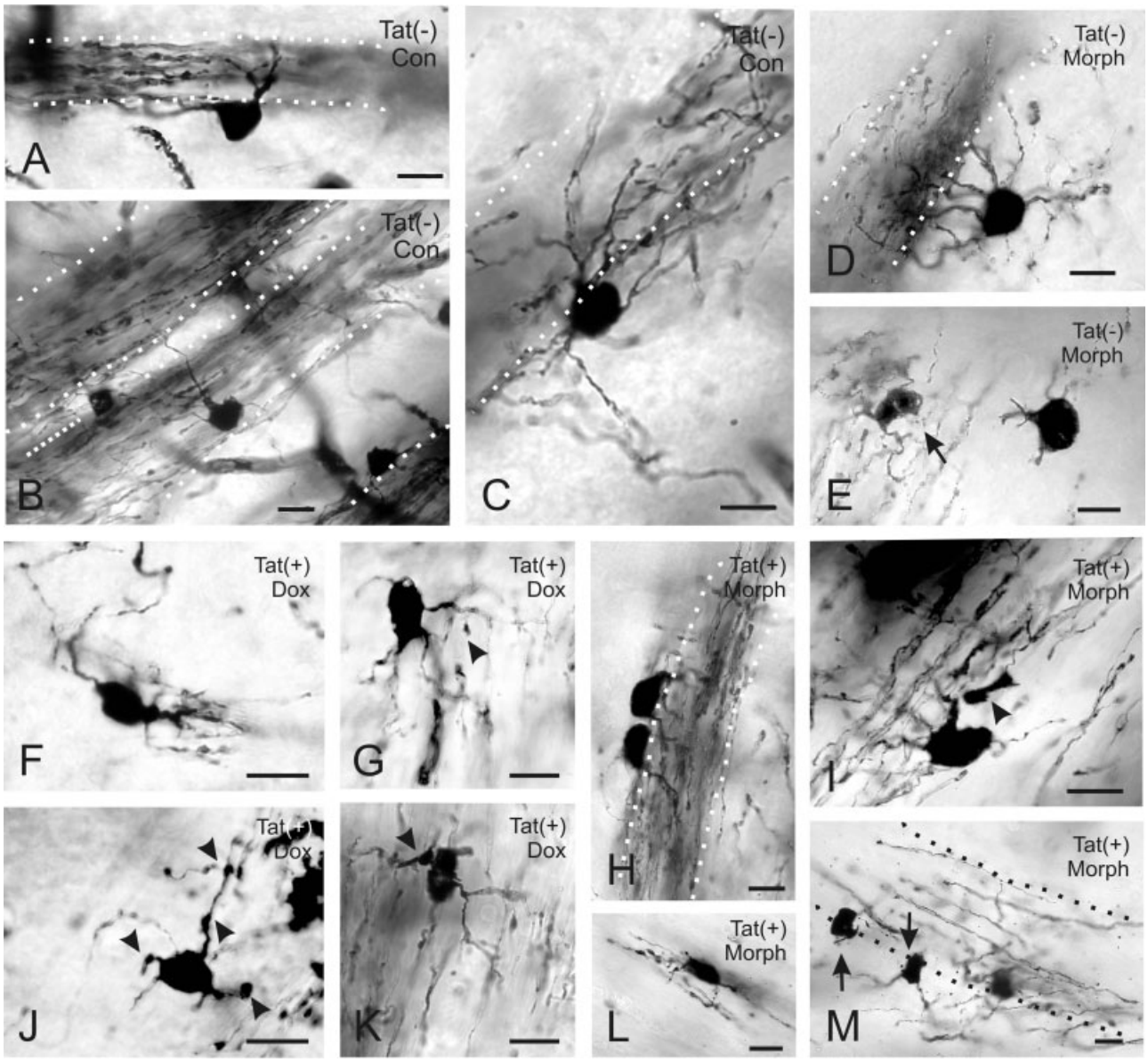

Fig. 5. Tat and morphine induce changes in OL morphology. Golgi–Kopsch impregnation was used to visualize the structure of OLs within the corpus callosum and striatum of Tat^+ and Tat^- mice undergoing various opiate treatments during a 7-day exposure to doxycycline (DOX). Sections were examined using a Zeiss Axio Observer microscope and multiple z-stack images were acquired through the same OL at 0.25–0.45 μm intervals. Z-stacks from the same OL were projected into a single, sharp two-dimensional image using the Zeiss AxioVision Extended Focus Module (see Methods for details). Brightfield photomicrographs (panels **A**–**M**) show cells from both Tat^+ and Tat^- mice, with treatment groups as labeled. Although normal appearing, myelinating OLs are present in both genotypes, there are increased examples of OLs with aberrant morphology in the Tat^+ mice. This is especially true in Tat^+ mice receiving treatments with DOX or DOX co-administered with morphine. Panels (A–C) show phenotypically normal OLs in the striatum and corpus callosum of wild type mice receiving unmodified chow. Most OLs in morphine-treated, wild type mice (D, E) displayed normal morphology (D). However, it was more common than usual to see smaller OLs that were potentially degenerating or regenerating (arrow in E), and OLs with phenotypic abnormalities such as severely stunted processes (cell in E without arrow). Expression of the HIV-1 Tat gene dramatically increased the presence of OLs with abnormal processes or cell bodies (F, G, J, K), and combined morphine exposure and Tat induction further aggravated the pathology (H, I, L, M). Pathologic changes included abnormal varicosities along processes or large, club-like cytoplasmic endings that could be several microns in diameter (arrowheads in G, I, J, K) and/or quantitative reductions in the number and extent of cytoplasmic processes (E–G, J, L, M). Note that diminished myelin contributions per cell were frequently associated with white matter tracts within the striatum following Tat induction, and especially when morphine was co-administered (M). It is important to note that despite overt pathologic changes accompanying Tat expression, many OLs appeared relatively normal indicating a nonuniform response among cells (H); arrowheads indicate abnormal cytoplasmic/myelin processes, arrows indicate apparent degenerating cells, dashed-lines indicate approximate boundaries of white matter tracts in the striatum; scale bars = 10 μm.

for neurons, astroglia, and microglia (Bruce-Keller et al., 2008; El-Hage et al., 2005, 2006b; Gurwell et al., 2001). Subpopulations of both glial progenitors and OLs express several types of opioid receptors, suggesting that they might be subject to opiate-induced synergism. Our initial *in vitro* studies showed that exposure of young, O_4^+ OLs to Tat alone or morphine alone caused an increased immunohistochemical expression of active cas-

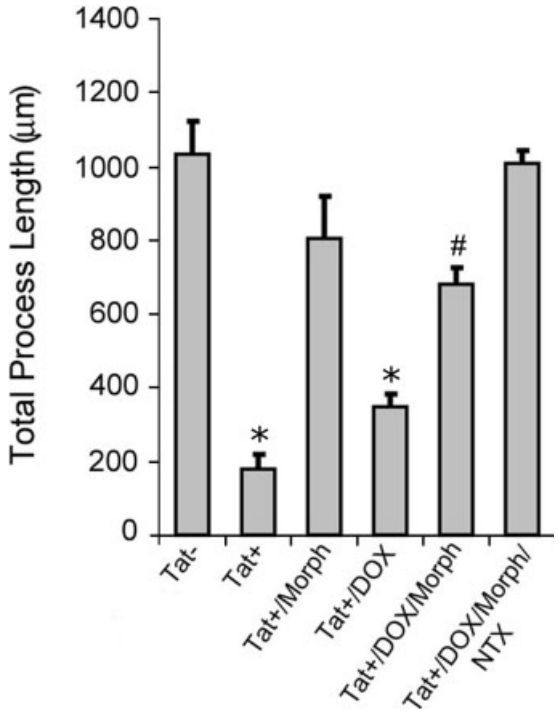

Fig. 6. The total length of all cell processes was measured in random, well impregnated OLs within the corpus callosum. This total length averaged 1,000 μm per OL in mice without the Tat transgene (Tat^-), but was reduced significantly in mice with the Tat transgene (Tat^+) regardless of the presence of doxycycline (DOX) (ANOVA; $^*P < 0.05$ vs. Tat^-, Tat^+/Morph, Tat^+/DOX/Morph, Tat^+/DOX/Morph/NTX). This finding of reduced process length in Tat^+ mice without DOX induction suggests that the DOX-induced promoter has some constitutive activity. Morphine dampens this response in Tat^+ mice both with and without DOX ($^*P < 0.05$ vs Tat^+/Morph, Tat^+/DOX/Morph), although overall process length in the Tat^+/DOX/Morph group is still significantly less than in the Tat^- group ($^{\#}P < 0.05$ vs. Tat^-). The dose of NTX used (60 mg/100 μL 50% DMSO) did not block the morphine effect. This may reflect the action of NTX on multiple opioid receptors, as well as endogenous secretion of multiple opioid peptides by OLs, as discussed in the text.

pase-3. When exposed simultaneously, the effect was additive and additivity was blocked by the opioid antagonist naloxone (Fig. 2). This led to a further examination of potential toxic and other effects *in vivo*, using transgenic mice that conditionally express HIV-1 $Tat_{1\text{-}86}$ in astroglia. We examined activation of caspase-3, a proapoptotic protease associated with release of caspase-activated DNAse and terminal DNA fragmentation. However, since our lab and others have shown that caspase-3 can be activated to high levels in situations where cells do not die (Adjan et al., 2007; Campbell and Holt, 2003; Garrido and Kroemer, 2004; Jarskog et al., 2007; Launay et al., 2005; McLaughlin, 2004; Oomman et al., 2004, 2005; Yang et al., 2004a,b), we additionally examined TUNEL labeling as a more unambiguous indicator of cell death. We also measured the arborization of OL processes as an index of whether Tat and/or morphine might cause nonlethal changes that impact OL function. Our results showed that all parameters had a clear-cut response to Tat and/or morphine. These responses were very endpoint specific, varying in sensitivity and threshold, and suggesting that a complex set of signaling responses is initiated by Tat and morphine exposure. All groups of Tat^+ mice, even those that were not exposed to DOX, showed significant upregulation of caspase-3 expression versus all Tat^- groups in APC+ OLs (Fig. 3). This likely indicates some constitutive expression of Tat due to promoter "leakiness," especially since OLs in Tat^+ mice also displayed changes in overall process length prior to DOX exposure (Fig. 6). Tat mRNA transcripts and immunostaining had previously been detected at low levels in the absence of DOX in a similar transgenic mouse (Kim et al., 2003). Of great interest, OLs from the same Tat^+ mice with upregulated active caspase-3 expression showed no increase in TUNEL labeling, except when treated with both DOX and morphine (Fig. 4). This suggests that caspase-3 expression did not necessarily lead to cell death. Further, it shows that Tat and morphine have additive effects on OLs *in vivo*, as previously described in the brain and/or *in vitro* for neurons (Gurwell et al., 2001; Hu et al., 2005; Turchan-Cholewo et al., 2006), astroglia (El-Hage et al., 2005, 2006a,b; Khurdayan et al., 2004) and microglia (Chao et al., 1994; El-Hage et al., 2006b). It is not clear whether all cells in the OL lineage are equally affected, since APC staining does not distinguish between mature and immature stages.

The small amounts of Tat that are constitutively released over the lifetime of Tat^+ mice appear to have a profound effect to reduce the average total process network in OLs (Fig. 6). Induction with DOX for 7 days does not increase this effect, suggesting an ongoing response at a very low threshold of sensitivity. This reduction might be due to the actual retraction or loss of processes in mature cells. However, it could also reflect a population of less well-arborized OLs whose differentiation has been compromised, or a proportional increase in a population of more immature OLs. The effects of Tat on glial population dynamics are of great interest and are under investigation. The ability to maintain multiple, myelinating processes that ensheathe an adequate number of axons is fundamental to OL function. Thus, while not a lethal response in itself, a reduction in process formation might seriously impact OL function.

Morphine co-administration seemed to mitigate some of the Tat effect on OL process length. This is contrary to our observations for caspase-3 and TUNEL in OLs, and for other endpoints in astrocytes and microglia, where morphine generally exacerbates the effect of Tat alone. Although morphine might be stabilizing OL processes or encouraging outgrowth, there is also a possibility that the population has been shifted toward larger cells with a larger process network through toxic effects directed toward immature OLs and/or their progenitors.

It is difficult to explain why the opiate antagonist NTX did not completely reverse the observed effects of morphine on all outcome measures. It did reverse morphine effects on caspase-3 *in vitro* (Fig. 2), and *in vivo* (Fig. 3), and significantly attenuated TUNEL effects (Fig. 4). However, when total OL process length was

measured after DOX ± morphine ± NTX after a slightly longer treatment period, the robust effect of morphine to antagonize Tat effects, in the absence and presence of DOX, was not reversed by NTX (Fig. 6). Although there are potential explanations for this observation, it may be extremely difficult to convincingly prove or disprove any of them, because opioids can modulate normal OL development. OLs express all major opioid receptors (Knapp et al., 1998, 2001; Stiene-Martin et al., 2001; Tryoen-Toth et al., 2000) and in addition synthesize KOR and DOR selective peptides (dynorphins, proenkephalins) (Knapp et al., 2001). KOR and MOR agonists have documented effects on OL differentiation and survival (Knapp and Hauser, 1996; Knapp et al., 1998, 2001; Sanchez et al., 2008). Although total process length reflects the process outgrowth of individual cells, it also reflects population shifts due to net changes in OL survival or maturation. For example, if mature OLs represent less of the total population, either because they die, or because there is increased progenitor formation, then average arborization may decrease. Vice versa, if there are proportionately more mature OLs, average total process length may increase. Since neither morphine nor NTX are entirely selective for particular opiate receptor types, both compounds have the potential to interfere with multiple endogenous opioid signals that affect measurements of average OL process length. Thus, one possible explanation for the paradoxical effects of NTX in this study is related to the complexity of opioid signaling in OLs. A broad-spectrum opioid receptor antagonist like NTX may disrupt endogenous opioid interactions that affect OL survival and differentiation and have effects unrelated to blocking exogenous morphine. Competing effects mediated through multiple opioid signaling pathways that converge on the same endpoint could mask NTX effects at MORs. Studies with more specific agonists and antagonists might not clarify this situation, since long-term exposure would almost certainly disrupt normal OL function. For now, the mechanism behind this particular result with NTX remains an unresolved point.

Lastly, some caution should be exercised when interpreting studies such as this with long-term exposure to opiates. Although NTX completely blocks morphine's acute effects (Bruce-Keller et al., 2008; El-Hage et al., 2006a,b), chronic administration of NTX, in general, adaptively increases opioid peptides and receptors, and can alter coupling to second messenger systems, thus modifying the response to morphine (Christie, 2008). Chronic morphine administration itself causes a decline in MOR signaling due to tolerance and dependence, while concurrently upregulating DOR and altering receptor heterodimerization (Cahill et al., 2001; Rozenfeld and Devi, 2007). These and other chronic, adaptive changes will likely alter cellular responses to morphine and NTX in unpredictable ways.

At one level, finding that OLs were sensitive to the Tat protein was unexpected, since earlier work in HIV patients showed no gross demyelination or reduction in myelin staining intensity in the CNS (Power et al., 1993). In similar immunoblotting studies to examine the abundance of CNS myelin basic protein, we found no differences between Tat^+ and Tat^- control mice. In light of the results showing OL abnormalities, several possibilities are suggested. Tat and/or morphine exposure may affect OL process formation and caspase-3/TUNEL expression, but those effects may not disrupt myelination or reduce myelin protein levels to an extent detected by immunoblotting or staining. These more subtle changes might still disrupt normal OL-axon relationships and eventually perturb neuron function. OL loss or aberrant myelin production by some OLs might also be compensated by increased myelin production per cell, or by recruitment of cells from an adult progenitor pool. We did note a population of smaller OLs with fewer processes in the Tat^+ groups, and although we believe these to be OLs retracting their processes, some could also be immature OLs. It is not clear that results observed in the transgenic mice are all due to direct actions of Tat and/or morphine on OLs, but cell culture studies do show that Tat/morphine can directly activate caspase-3 within OLs. And while the effects of Tat and morphine on OL lineage cells could be mouse-specific, this seems unlikely since the majority of effects observed for astroglia, microglia, and CNS neurons in the Tat transgenic model bears out what is believed to be the situation in the human disease.

What meaning do the present results have in terms of human disease and neurological function in HIV patients? White matter "pallor" has been frequently described on MRIs from HIV patients with neuroAIDs (Cherner et al., 2002; Glass et al., 1993; Gray et al., 1992, 1996; Lanjewar et al., 1998; McArthur et al., 1989; Schwartz and Major, 2006), although this has been attributed largely to edema associated with protein leakage through a compromised endothelium. Our results do not exclude this effect, but rather suggest that OLs are also direct and/or indirect targets of the Tat protein and/or inflammatory changes that Tat initiates within the brain. HAART treatment has improved the life expectancy of many HIV patients. In these patients, where the disease is a more chronic condition, the consequences of subtle changes in myelination over a longer time course may become a more important part of the clinical picture. Our previous work showed that Tat and opioids have synergistic effects on neurons, implying that concurrent opioid abuse by HIV patients may directly increase the risk of neurological deficits. The present results show that OLs are also vulnerable to this synergy, suggesting an additional basis for the prevalence of neuroAIDs among opioid users. We also noted that immature OLs derived from glial progenitor cultures were synergistically affected by exposure to Tat and morphine. These results extend our previous findings, which showed that more immature progenitors from cortex and spinal cord were targets of Tat and opioid toxicity (Buch et al., 2007; Khurdayan et al., 2004). Since glial production and myelination continue for several years after birth in humans, these findings on glial progenitors and young OLs may be particularly relevant to

pediatric HIV patients, who have a higher prevalence and accelerated rate of onset of neurological complications compared with adult HIV patients (Drotar and Olness, 1997; Ensoli and Wang, 1997; Schwartz and Major, 2006; Van Rie and Harrington, 2007). The adult CNS also contains a population of glial progenitors (Gensert and Goldman, 2001; Wolswijk and Noble, 1989), which might be vulnerable to HIV protein/opioid exposure. Studies to examine the response of glial progenitors to opiates and viral proteins at various developmental points in both the immature and mature CNS are currently underway.

Overall, our results suggest that OLs are extremely sensitive to HIV-1 Tat exposure. The consequences of Tat exposure can be either selectively exacerbated or alleviated by concurrent administration of morphine, depending upon the endpoint in question. Tat and opioid signaling may thus be integrated through convergence on multiple signaling pathways within OLs. When active caspase-3 expression and process length were used as endpoints, OLs were sensitive even to the low levels of Tat produced without DOX induction. We have not seen this in other CNS cells studied in these transgenic mice, including astroglia, striatal neurons and microglia/monocytes, using any of several endpoints (Bruce-Keller et al., 2008) (Knapp and Hauser, unpublished data). Thus OLs, in contrast to other CNS cell types, are either more sensitive to low levels of Tat or do not habituate as readily to its presence. Assuming that OLs in the human CNS behave similarly, the endpoints that we have studied suggest a deleterious effect of Tat exposure on OLs, and thus on OL-neuron relationships, in both the adult and developing CNS. The Tat and morphine effects on OLs described in our studies may provide an alternative or additional explanation for white matter abnormalities observed in some HIV patients. As HAART treatment lengthens survival time, functional changes due to altered glial populations may contribute increasingly to the neurological complications observed in HIV patients, and especially in those exposed to opioid drugs of abuse.

ACKNOWLEDGMENTS

The authors thank Mr. Evan Mussetter, Mr. Anthony Mullins, and Ms. Yelena Alimova for technical assistance.

REFERENCES

Adjan VV, Hauser KF, Bakalkin G, Yakovleva T, Gharibyan A, Scheff SW, Knapp PE. 2007. Caspase-3 activity is reduced after spinal cord injury in mice lacking dynorphin: Differential effects on glia and neurons. Neuroscience 148:724–736.

Aksenov MY, Hasselrot U, Wu G, Nath A, Anderson C, Mactutus CF, Booze RM. 2003. Temporal relationships between HIV-1 Tat-induced neuronal degeneration, OX-42 immunoreactivity, reactive astrocytosis, and protein oxidation in the rat striatum. Brain Res 987:1–9.

Ances BM, Ellis RJ. 2007. Dementia and neurocognitive disorders due to HIV-1 infection. Semin Neurol 27:86–92.

Anthony IC, Arango JC, Stephens B, Simmonds P, Bell JE. 2008. The effects of illicit drugs on the HIV infected brain. Front Biosci 13: 1294–1307.

Anthony IC, Bell JE. 2008. The neuropathology of HIV/AIDS. Int Rev Psychiatry 20:15–24.

Arnot MI, Bateson AN, Martin IL. 1996. Dimethyl sulfoxide/propylene glycol is a suitable solvent for the delivery of diazepam from osmotic minipumps. J Pharmacol Toxicol Methods 36:29–31.

Bell JE, Arango JC, Anthony IC. 2006. Neurobiology of multiple insults: HIV-1-associated brain disorders in those who use illicit drugs. J Neuroimmune Pharmacol 1:182–191.

Bhat RV, Axt KJ, Fosnaugh JS, Smith KJ, Johnson KA, Hill DE, Kinzler KW, Baraban JM. 1996. Expression of the APC tumor suppressor protein in oligodendroglia. Glia 17:169–174.

Bonavia R, Bajetto A, Barbero S, Albini A, Noonan DM, Schettini G. 2001. HIV-1 Tat causes apoptotic death and calcium homeostasis alterations in rat neurons. Biochem Biophys Res Commun 288:301–308.

Bruce-Keller AJ, Turchan-Cholewo J, Smart EJ, Geurin T, Chauhan A, Ried R, Xu R, Nath A, Knapp PE, Hauser KF. 2008. Morphine causes rapid increases in glial activation and neuronal injury in the striatum of inducible HIV-1 Tat transgenic mice. Glia 56:1414–1427.

Buch SK, Khurdayan VK, Lutz SE, Knapp PE, El-Hage N, Hauser KF. 2007. Glial-restricted precursors: Patterns of expression of opioid receptors and relationship to HIV-1 Tat and morphine susceptibility in vitro. Neuroscience 146:1546–1554.

Burdo TH, Katner SN, Taffe MA, Fox HS. 2006. Neuroimmunity, drugs of abuse, and neuroAIDS. J Neuroimmune Pharmacol 1:41–49.

Cahill CM, Morinville A, Lee MC, Vincent JP, Collier B, Beaudet A. 2001. Prolonged morphine treatment targets delta opioid receptors to neuronal plasma membranes and enhances delta-mediated antinociception. J Neurosci 21:7598–7607.

Campbell DS, Holt CE. 2003. Apoptotic pathway and MAPKs differentially regulate chemotropic responses of retinal growth cones. Neuron 37:939–952.

Carr DJ, France CP. 1993. Immune alterations in chronic morphine-treated rhesus monkeys. Adv Exp Med Biol 335:35–39.

Chao CC, Gekker G, Sheng WS, Hu S, Tsang M, Peterson PK. 1994. Priming effect of morphine on the production of tumor necrosis factor-α by microglia: Implications in respiratory burst activity and human immunodeficiency virus-1 expression. J Pharmacol Exp Ther 269:198–203.

Cherner M, Masliah E, Ellis RJ, Marcotte TD, Moore DJ, Grant I, Heaton RK. 2002. Neurocognitive dysfunction predicts postmortem findings of HIV encephalitis. Neurology 59:1563–1567.

Christie MJ. 2008. Cellular neuroadaptations to chronic opioids: Tolerance, withdrawal and addiction. Br J Pharmacol 154:384–396.

Cysique LA, Maruff P, Brew BJ. 2004. Prevalence and pattern of neuropsychological impairment in human immunodeficiency virus-infected/acquired immunodeficiency syndrome (HIV/AIDS) patients across pre- and post-highly active antiretroviral therapy eras: A combined study of two cohorts. J Neurovirol 10:350–357.

Donahoe RM, Falek A. 1988. Neuroimmunomodulation by opiates and other drugs of abuse: Relationship to HIV infection and AIDS. Adv Biochem Psychopharmacol 44:145–158.

Drotar D, Olness K, Wiznitzer M, Guay L, Marum L, Svilar G, Hom D, Fagan JF, Ndugwa C, Kiziri-Mayengo R. 1997. Neurodevelopmental outcomes of Ugandan infants with human immunodeficiency virus type 1 infection. Pediatrics 100:E5.

El-Hage N, Gurwell JA, Singh IN, Knapp PE, Nath A, Hauser KF. 2005. Synergistic increases in intracellular Ca^{2+}, and the release of MCP-1, RANTES, and IL-6 by astrocytes treated with opiates and HIV-1 Tat. Glia 50:91–106.

El-Hage N, Wu G, Ambati J, Bruce-Keller AJ, Knapp PE, Hauser KF. 2006a. CCR2 mediates increases in glial activation caused by exposure to HIV-1 Tat and opiates. J Neuroimmunol 178:9–16.

El-Hage N, Wu G, Wang J, Ambati J, Knapp PE, Reed J, Bruce-Keller A, Hauser KF. 2006b. HIV Tat1-72 and opiate-induced changes in astrocytes promote chemotaxis of microglia through the expression of MCP-1 and alternative chemokines. Glia 53:132–146.

Ensoli F, Wang H, Fiorelli V, Zeichner SL, De Cristofaro MR, Luzi G, Thiele CJ. 1997. HIV-1 infection and the developing nervous system: lineage-specific regulation of viral gene expression and replication in distinct neuronal precursors. J Neurovirol 3:290–298.

Feng P, Rahim RT, Cowan A, Liu-Chen LY, Peng X, Gaughan J, Meissler JJ Jr, Adler MW, Eisenstein TK. 2006. Effects of μ, κ or δ opioids administered by pellet or pump on oral Salmonella infection and gastrointestinal transit. Eur J Pharmacol 534:250–257.

Fitting S, Booze RM, Hasselrot U, Mactutus CF. 2008. Differential long-term neurotoxicity of HIV-1 proteins in the rat hippocampal formation: A design-based stereological study. Hippocampus 18:135–147.

Garrido C, Kroemer G. 2004. Life's smile, death's grin: Vital functions of apoptosis-executing proteins. Curr Opin Cell Biol 16:639–646.

Gensert JM, Goldman JE. 2001. Heterogeneity of cycling glial progenitors in the adult mammalian cortex and white matter. J Neurobiol 48:75–86.

Ghafouri M, Amini S, Khalili K, Sawaya BE. 2006. HIV-1 associated dementia: Symptoms and causes. Retrovirology 3:28.

Glass JD, Wesselingh SL, Selnes OA, McArthur JC. 1993. Clinical-neuropathologic correlation in HIV-associated dementia. Neurology 43:2230–2237.

Gonzalez E, Rovin BH, Sen L, Cooke G, Dhanda R, Mummidi S, Kulkarni H, Bamshad MJ, Telles V, Anderson SA, Walter EA, Stephan KT, Deucher M, Mangano A, Bologna R, Ahuja SS, Dolan MJ, Ahuja SK. 2002. HIV-1 infection and AIDS dementia are influenced by a mutant MCP-1 allele linked to increased monocyte infiltration of tissues and MCP-1 levels. Proc Natl Acad Sci USA 99:13795–13800.

Gonzalez-Scarano F, Martin-Garcia J. 2005. The neuropathogenesis of AIDS. Nat Rev Immunol 5:69–81.

Gray F, Lescs MC, Keohane C, Paraire F, Marc B, Durigon M, Gherardi R. 1992. Early brain changes in HIV infection: Neuropathological study of 11 HIV seropositive, non-AIDS cases. J Neuropathol Exp Neurol 51:177–185.

Gray F, Scaravilli F, Everall I, Chretien F, An S, Boche D, Adle-Biassette H, Wingertsmann L, Durigon M, Hurtrel B, Chiodi F, Bell J, Lantos P. 1996. Neuropathology of early HIV-1 infection. Brain Pathol 6:1–15.

Gurwell JA, Nath A, Sun Q, Zhang J, Martin KM, Chen Y, Hauser KF. 2001. Synergistic neurotoxicity of opioids and human immunodeficiency virus-1 Tat protein in striatal neurons in vitro. Neuroscience 102:555–563.

Hauser KF, El-Hage N, Stiene-Martin A, Maragos WF, Nath A, Persidsky Y, Volsky DJ, Knapp PE. 2007. HIV-1 neuropathogenesis: Glial mechanisms revealed through substance abuse. J Neurochem 100: 567–586.

Hauser KF, McLaughlin PJ, Zagon IS. 1989. Endogenous opioid systems and the regulation of dendritic growth and spine formation. J Comp Neurol 281:13–22.

Hu S, Sheng WS, Lokensgard JR, Peterson PK. 2005. Morphine potentiates HIV-1 gp120-induced neuronal apoptosis. J Infect Dis 191:886–889.

Jana A, Pahan K. 2004. Human immunodeficiency virus type 1 gp120 induces apoptosis in human primary neurons through redox-regulated activation of neutral sphingomyelinase. J Neurosci 27:9531–9540.

Jarskog LF, Gilmore JH, Glantz LA, Gable KL, German TT, Tong RI, Lieberman JA. 2007. Caspase-3 activation in rat frontal cortex following treatment with typical and atypical antipsychotics. Neuropsychopharmacology 32:95–102.

Jones GJ, Barsby NL, Cohen EA, Holden J, Harris K, Dickie P, Jhamandas J, Power C. 2007. HIV-1 Vpr causes neuronal apoptosis and in vivo neurodegeneration. J Neurosci 27:3703–3711.

Kandanearatchi A, Williams B, Everall IP. 2003. Assessing the efficacy of highly active antiretroviral therapy in the brain. Brain Pathol 13:104–110.

Khurdayan VK, Buch S, El-Hage N, Lutz SE, Goebel SM, Singh IN, Knapp PE, Turchan-Cholewo J, Nath A, Hauser KF. 2004. Preferential vulnerability of astroglia and glial precursors to combined opioid and HIV-1 Tat exposure in vitro. Eur J Neurosci 19:3171–3182.

Kim BO, Liu Y, Ruan Y, Xu ZC, Schantz L, He JJ. 2003. Neuropathologies in transgenic mice expressing human immunodeficiency virus type 1 Tat protein under the regulation of the astrocyte-specific glial fibrillary acidic protein promoter and doxycycline. Am J Pathol 162:1693–1707.

Knapp PE, Hauser KF. 1996. m-Opioid receptor activation enhances DNA synthesis in immature oligodendrocytes. Brain Res 743:341–345.

Knapp PE, Itkis OS, Zhang L, Spruce BA, Bakalkin G, Hauser KF. 2001. Opiate signaling in oligodendrocytes: Possible autocrine effects on cell survival and development. Glia 35:156–165.

Knapp PE, Maderspach K, Hauser KF. 1998. Endogenous opioid system in developing normal and jimpy oligodendrocytes: m and k opioid receptors mediate differential mitogenic and growth responses. Glia 22:189–201.

Kopnisky KL, Bao J, Lin YW. 2007. Neurobiology of HIV, psychiatric and substance abuse comorbidity research: Workshop report. Brain Behav Immun 21:428–441.

Kruman II, Nath A, Mattson MP. 1998. HIV-1 protein Tat induces apoptosis of hippocampal neurons by a mechanism involving caspase activation, calcium overload, and oxidative stress. Exp Neurol 154:276–288.

Langford TD, Letendre SL, Larrea GJ, Masliah E. 2003. Changing patterns in the neuropathogenesis of HIV during the HAART era. Brain Pathol 13:195–210.

Lanjewar DN, Jain PP, Shetty CR. 1998. Profile of central nervous system pathology in patients with AIDS: An autopsy study from India. AIDS 12:309–313.

Launay S, Hermine O, Fontenay M, Kroemer G, Solary E, Garrido C. 2005. Vital functions for lethal caspases. Oncogene 24:5137–5148.

Li Y, Merrill JD, Mooney K, Song L, Wang X, Guo CJ, Savani RC, Metzger DS, Douglas SD, Ho WZ. 2003. Morphine enhances HIV infection of neonatal macrophages. Pediatr Res 54:282–288.

Ligon KL, Fancy SP, Franklin RJ, Rowitch DH. 2006. Olig gene function in CNS development and disease. Glia 54:1–10.

Lipton SA. 1997. Neuropathogenesis of acquired immunodeficiency syndrome dementia. Curr Opin Neurol 10:247–253.

Mahajan SD, Aalinkeel R, Reynolds JL, Nair BB, Fernandez SF, Schwartz SA, Nair MP. 2005. Morphine exacerbates HIV-1 viral protein gp120 induced modulation of chemokine gene expression in U373 astrocytoma cells. Curr HIV Res 3:277–288.

McArthur JC, Becker PS, Parisi JE, Trapp B, Selnes OA, Cornblath DR, Balakrishnan J, Griffin JW, Price D. 1989. Neuropathological changes in early HIV-1 dementia. Ann Neurol 26:681–684.

McLaughlin B. 2004. The kinder side of killer proteases: Caspase activation contributes to neuroprotection and CNS remodeling. Apoptosis 9:111–121.

Nath A, Anderson C, Jones M, Maragos W, Booze R, Mactutus C, Bell J, Hauser KF, Mattson M. 2000. Neurotoxicity and dysfunction of dopaminergic systems associated with AIDS dementia. J Psychopharmacol 14:222–227.

Nath A, Hauser KF, Wojna V, Booze RM, Maragos W, Prendergast M, Cass W, Turchan JT. 2002. Molecular basis for interactions of HIV and drugs of abuse. J Acquir Immune Defic Syndr 31(Suppl 2):S62–S69.

Nath A, Psooy K, Martin C, Knudsen B, Magnuson DS, Haughey N, Geiger JD. 1996. Identification of a human immunodeficiency virus type 1 Tat epitope that is neuroexcitatory and neurotoxic. J Virol 70:1475–1480.

Neuenburg JK, Brodt HR, Herndier BG, Bickel M, Bacchetti P, Price RW, Grant RM, Schlote W. 2002. HIV-related neuropathology, 1985 to 1999: rising prevalence of HIV encephalopathy in the era of highly active antiretroviral therapy. J Acquir Immune Defic Syndr 31:171–177.

Noel RJ Jr, Kumar A. 2006. Virus replication and disease progression inversely correlate with SIV tat evolution in morphine-dependent and SIV/SHIV-infected Indian rhesus macaques. Virology 346:127–138.

Oomman S, Finckbone V, Dertien J, Attridge J, Henne W, Medina M, Mansouri B, Singh H, Strahlendorf H, Strahlendorf J. 2004. Active caspase-3 expression during postnatal development of rat cerebellum is not systematically or consistently associated with apoptosis. J Comp Neurol 476:154–173.

Oomman S, Strahlendorf H, Finckbone V, Strahlendorf J. 2005. Nonlethal active caspase-3 expression in Bergmann glia of postnatal rat cerebellum. Brain Res Dev Brain Res 160:130–145.

Patel CA, Mukhtar M, Pomerantz RJ. 2000. Human immunodeficiency virus type 1 Vpr induces apoptosis in human neuronal cells. J Virol 74:9717–9726.

Peart JN, Gross GJ. 2004. Morphine-tolerant mice exhibit a profound and persistent cardioprotective phenotype. Circulation 109:1219–1222.

Peterson PK, Gekker G, Hu S, Cabral G, Lokensgard JR. 2004. Cannabinoids and morphine differentially affect HIV-1 expression in CD4(+) lymphocyte and microglial cell cultures. J Neuroimmunol 147:123–126.

Peterson PK, Molitor TW, Chao CC. 1993. Mechanisms of morphine-induced immunomodulation. Biochem Pharmacol 46:343–348.

Power C, Kong PA, Crawford TO, Wesselingh S, Glass JD, McArthur JC, Trapp BD. 1993. Cerebral white matter changes in acquired immunodeficiency syndrome dementia: Alterations of the blood-brain barrier. Ann Neurol 34:339–350.

Rahim RT, Meissler JJ, Zhang L, Adler MW, Rogers TJ, Eisenstein TK. 2003. Withdrawal from morphine in mice suppresses splenic macrophage function, cytokine production, and costimulatory molecules. J Neuroimmunol 144:16–27.

Rozenfeld R, Devi LA. 2007. Receptor heterodimerization leads to a switch in signaling: β-Arrestin2-mediated ERK activation by μ-δ opioid receptor heterodimers. FASEB J 21:2455–2465.

Sanchez ES, Bigbee JW, Fobbs W, Robinson SE, Sato-Bigbee C. 2008. Opioid addiction and pregnancy: Perinatal exposure to buprenorphine affects myelination in the developing brain. Glia 56:1017–1027.

Schwartz L, Major EO. 2006. Neural progenitors and HIV-1-associated central nervous system disease in adults and children. Curr HIV Res 4:319–327.

Schweitzer C, Keller F, Schmitt MP, Jaeck D, Adloff M, Schmitt C, Royer C, Kirn A, Aubertin AM. 1991. Morphine stimulates HIV replication in primary cultures of human Kupffer cells. Res Virol 142:189–195.

Singh IN, Goody RJ, Dean C, Ahmad NM, Lutz SE, Knapp PE, Nath A, Hauser KF. 2004. Apoptotic death of striatal neurons induced by HIV-1 Tat and gp120: Differential involvement of caspase-3 and endonuclease G. J Neurovirol 10:141–151.

Sommer I, Schachner M. 1982. Cells that are O4 antigen-positive and O1 antigen-negative differentiate into O1 antigen-positive oligodendrocytes. Neurosci Lett 29:183–188.

Stiene-Martin A, Knapp PE, Martin K, Gurwell JA, Ryan S, Thornton SR, Smith FL, Hauser KF. 2001. Opioid system diversity in developing neurons, astroglia, and oligodendroglia in the subventricular zone and striatum: Impact on gliogenesis in vivo. Glia 36: 78–88.

Suzuki S, Carlos MP, Chuang LF, Torres JV, Doi RH, Chuang RY. 2002. Methadone induces CCR5 and promotes AIDS virus infection. FEBS Lett 519:173–177.

Trillo-Pazos G, McFarlane-Abdulla E, Campbell IC, Pilkington GJ, Everall IP. 2000. Recombinant nef HIV-IIIB protein is toxic to human neurons in culture. Brain Res 864:315–326.

Tryoen-Toth P, Gaveriaux-Ruff C, Labourdette G. 2000. Down-regulation of μ-opioid receptor expression in rat oligodendrocytes during their development in vitro. J Neurosci Res 60:10–20.

Turchan-Cholewo J, Liu Y, Gartner S, Reid R, Jie C, Peng X, Chen KC, Chauhan A, Haughey N, Cutler R, Mattson MP, Pardo C, Conant K, Sacktor N, McArthur JC, Hauser KF, Gairola C, Nath A. 2006. Increased vulnerability of ApoE4 neurons to HIV proteins and opiates: Protection by diosgenin and L-deprenyl. Neurobiol Dis 23:109–119.

Vallejo R, de Leon-Casasola O, Benyamin R. 2004. Opioid therapy and immunosuppression: A review. Am J Ther 11:354–365.

Van Rie A, Harrington PR, Dow A, Robertson K. 2007. Neurologic and neurodevelopmental manifestations of pediatric HIV/AIDS: a global perspective. Eur J Paediatr Neurol 11:1–9.

Wolswijk G, Noble M. 1989. Identification of an adult-specific glial progenitor cell. Development 105:387–400.

Woodruff RH, Tekki-Kessaris N, Stiles CD, Rowitch DH, Richardson WD. 2001. Oligodendrocyte development in the spinal cord and telencephalon: Common themes and new perspectives. Int J Dev Neurosci 19:379–385.

Yang JY, Michod D, Walicki J, Murphy BM, Kasibhatla S, Martin SJ, Widmann C. 2004a. Partial cleavage of RasGAP by caspases is required for cell survival in mild stress conditions. Mol Cell Biol 24:10425–10436.

Yang JY, Michod D, Walicki J, Widmann C. 2004b. Surviving the kiss of death. Biochem Pharmacol 68:1027–1031.